2015 International Symposium on Nonlinear Theory and its Applications
NOLTA2015, Kowloon, Hong Kong, China, December 1-4, 2015

Penetration of Helium Ions into Tungsten Material with Nanoporous Structure

Seiki Saito†, Kenta Yoshida†, and Hiroaki Nakamura‡

†Department of Electrical Engineering, National Institute of Technology, Kushiro College
2-32-1 Otanoshike-Nishi, Kushiro 084-0916, Japan
‡Department of Helical Plasma Research, National Institute for Fusion Science
322-6 Oroshi-cho, Toki 509-5292, Japan
Email: saitos@kushiro-ct.ac.jp

Abstract– Many experimental studies reported the surface modification of tungsten material under helium plasma irradiation. To investigate the effects of the structural modification to the penetration process of helium ions in atomic scale, binary-collision-approximation-based simulation of helium injection into tungsten material with nanoporous structure is performed.

1. Introduction

The largest international nuclear fusion device called ITER is currently under construction in Cadarache, France. In the fusion device, deuterium and tritium plasma is confined by magnetic fields. The temperature of the plasma becomes more than 100 million degrees Celsius. As a result of nuclear fusion of deuterium and tritium in ITER, helium ash is generated. The helium ash transports along magnetic force line and impacts to the divertor plates. Although the plasma temperature around the divertor plates is relatively low in the steady state operation, the helium ash injects into divertor plates with higher energy when transient thermal events such as disruption occur. The helium atoms are retained in the bulk of divertor plates after plasma irradiation. The retention of helium atoms affects the tolerance as plasma facing material.

Many experimental studies reported bubble formation on the surface of tungsten material under helium plasma irradiation [1-4]. Furthermore, a number of experiments show that helium plasma constructs filament (fuzz) structures [5, 6] whose diameter is in nanometer-scale on the tungsten material under the suitable condition (i.e., material temperature of 1000-2000 K and incident energy of 20–100 eV). The surface modification of divertor plates also affects the penetration and retention processes. For the steady-state operation of ITER, it is required to understand deeply the elementary processes of the helium penetration under plasma irradiation in atomic scale.

The penetration process of energetic incident ions in materials is often investigated by binary-collision-approximation-based (BCA) simulation code, for example ACAT [7], EDDY [8], ERO, TRIM [9] codes. In our previous research [10-14], we developed AC∀T code which was the extended ACAT code to handle any structure of target materials, including monocrystals, polycrystals, crystals with defects, and amorphous. In this study, therefore, we perform BCA simulation of helium injection into tungsten material by AC∀T code to investigate the penetration depth of incident helium ions.

2. Simulation Method [10, 11]

Figure 1 shows the schematic diagram of BCA simulation. A projectile is injected into a target material. The projectile collides with the nearest neighbor atom. The other interaction between surrounding atoms and the projectile is neglected in BCA simulation. The momentum of the projectile changes at the collision, then the projectile collides with the next target atom. In the collision process of BCA, the motion of target atoms which collide with the projectile depends on their received kinetic energy E_t. When E_t is lower than the binding energy E_b of the target atom, the target atom dose not move. On the other hand, when E_t is larger than E_b, the target atom recoils. The motion of recoil atoms is solved in the same way as the projectile. The scattering angle of the projectile and the target atoms at each collision are obtained analytically in a two-body interatomic potential $V(r)$, where r is the distance between the projectile and the target atom. In our BCA code named AC∀T, the Moliere approximation to the Thomas-Fermi potential [15] is employed.

3. Simulation Model

Simulation of helium injection into tungsten material is performed by AC∀T code. The size of target material is set to 158.0 Å×15.8 Å×1580.0 Å, as shown in Fig. 2. The tungsten atoms are arranged as bcc crystal with the lattice constant of 3.16 Å. The length of a size of cell is set to the half of the lattice constant, therefore the target material consists of 100×10×1000 cells. The z-axis of the simulation box is set parallel to the edge of the target material whose length is 1580.0 Å. Periodic boundary conditions are used in x- and y-directions. The initial temperature of the target material is set to 0 K. A total of 100,000 helium atoms are injected one by one into the target material. The incident energy of helium atoms are fixed to 500 eV. The incident angle is set to parallel to z-axis, i.e., perpendicular to (100) surface of bcc crystal.

The x- and y-coordinates of the starting positions of the helium atoms are set randomly.

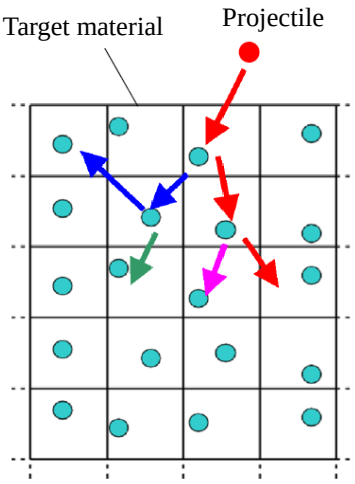

Fig. 1. Schematic diagram of binary collision approximation. [11]

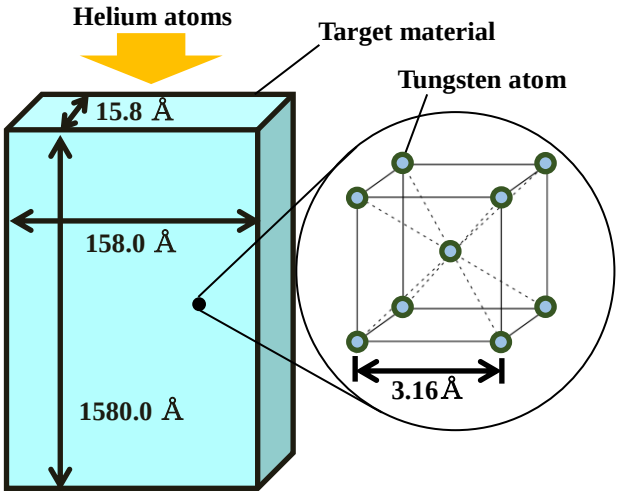

Fig. 2. Schematic diagram of system of our simulation.

To make nanoporous structure of tungsten material, many holes are generated near the surface by removing the tungsten atoms in spheres whose diameter is 10.0 Å. Figure 3 shows the example of the surface of target material which has 50 holes. The center positions of holes are distributed as Gaussian function $N(\mu=0$ Å, $\sigma^2=50^2$ Å$^2)$ in z-direction, while they are uniformly distributed in x- and y-direction. The total number of holes are set as a parameter up to 1000. The dependence of mean penetration depth for 100,000 helium atoms on the number of holes is investigate in this study.

4. Simulation Results

Figure 4 shows the graph of mean penetration depth against the number of holes. It is clear that the mean penetration depth decreases as the number of holes increases although the surface of target material becomes less dense. Moreover, the slope of the graph becomes smaller as the number of holes increases. The reasons of the two facts are discussed in the next section.

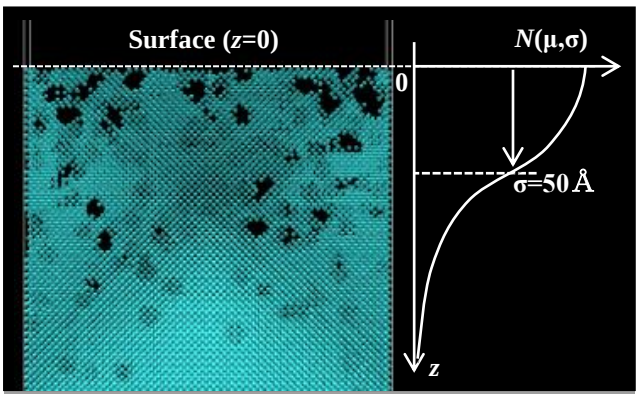

Fig. 3. Target material with holes.

5. Discussion

To investigate the dependence of the slope of mean penetration depth on the number of holes, we estimate the surface area of target material. The surface becomes wider as the number of holes increases. However, the surface area is not proportional to the number of holes because the area where two holes are overlapped increases as the number of holes increases as shown in Fig. 5. By calculating the surface area, it is possible to remove the effect of the increase of overlapped area from the dependence.

To estimate the surface area of target material, all atoms located near the surface boundary of target material are detected. Figure 6 shows the method of the detection of the surface atoms. In order to determine whether an atom is located at the surface or not, a sphere, whose center is located at the positon of the atom and the radius is r_e = 4 Å, is considered. In the case of perfect bcc tungsten

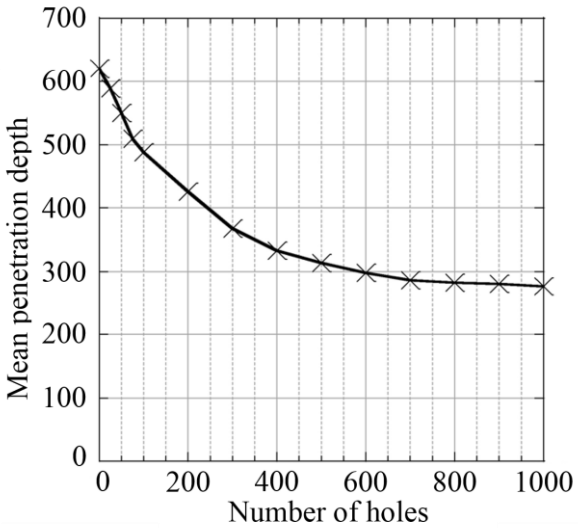

Fig. 4. Dependence of mean penetration depth on the number of holes.

crystal with the lattice constant of 3.16 Å, 15 atoms are located in the sphere in the case of the atom in the bulk of the target material (i.e. represented by the blue balls in Fig. 6). However fewer atoms are located in the sphere in the case of atoms near the surface (i.e. represented by the red balls in Fig. 6). Therefore, surface atoms can be detected when the number of atoms in the sphere is fewer than 15. Figure 7 (b) shows the result of detection. White dots denote the atoms which are detected as the surface atoms. In the case of Fig. 7 (b), N_b=2854 tungsten atoms are detected as surface atoms. Figure 7 (a) shows the result obtained by the same procedure for the case of perfect crystalline structure. In the case of perfect crystalline structure, only N_a=250 tungsten atoms of first layer of material are detected as the surface atoms. The surface area S_a of Fig. 7 (a) case is equal to 15.8 Å × 158.0 Å=2496.4 Å^2. By multiplying the ratio N_b/N_a to the surface area S_a of Fig. 7 (a), the surface area of Fig. 7 (b) can be estimated as S_b=28498.9 Å^2.

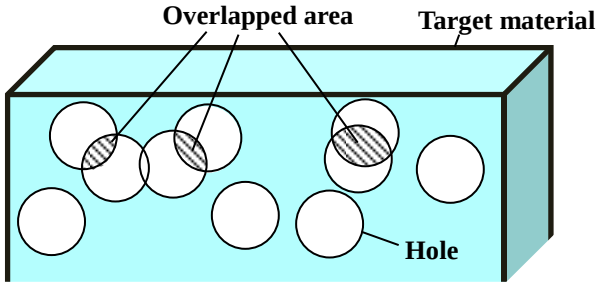

Fig. 5. Schematic diagram of overlapped area of holes.

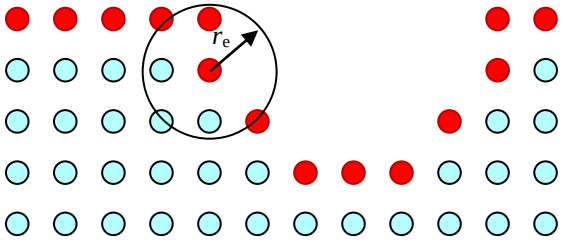

Fig. 6. Detection of atoms on the surface the boundary of target material.

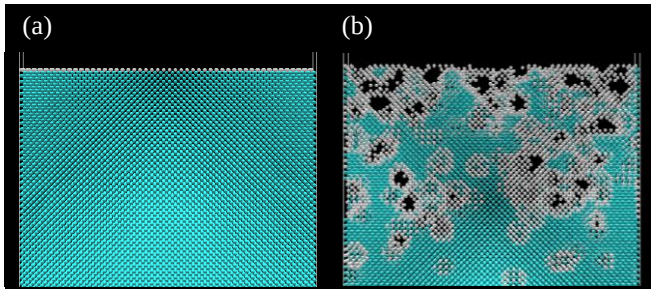

Fig. 7. Results of detection of surface boundary. White dots denote the atoms detected as boundary.

Figure 8 shows the graph of relation between number of holes and the surface area calculated by the above mentioned method. As we mentioned before, the surface area is not proportional to the number of holes. As increase the number of holes, the slope of Fig. 8 decreases because the overlapped area of holes increases. Figure 9 shows the graph of the mean penetration depth against the surface area. From this figure, it is clearly seen that the mean penetration depth proportionally decreases as the surface area increases. Therefore, it is concluded that the decrease of the slope of Fig. 4 is caused by the increase of overlapped area of holes.

To investigate the reason of the decrease of mean penetration depth against the increase of surface area in detail, we carefully observed the trajectory of each incident helium atom. From the observation, it is discovered that the decrease of mean penetration depth is caused by the channeling effect at holes. The

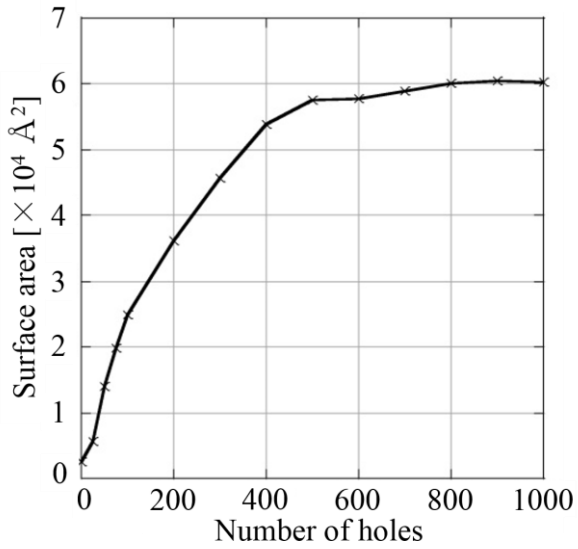

Fig. 8. Relation between the surface area and number of holes.

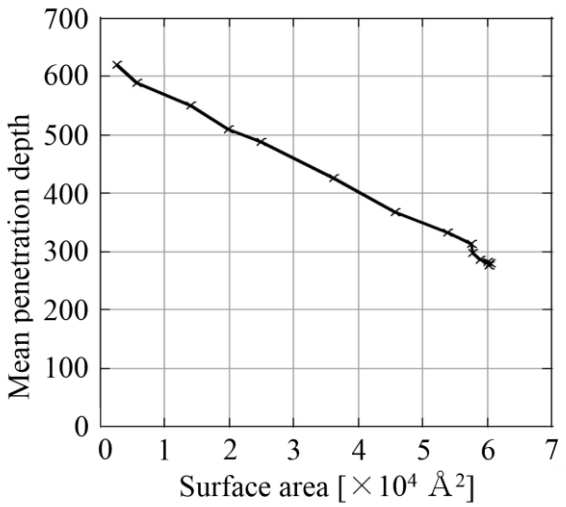

Fig. 9. Surface area dependence of mean penetration depth.

channeling is the phenomenon that incident atoms with specific incident angle corresponding to crystalline structure move straightly without causing large angle scattering in the target material. It is known that the channeling is mainly caused when the scattering angle of the first collision is smaller than $\tan^{-1}(1/2)$ as shown in Fig. 10 [13]. Therefore, the many incident helium atoms move straightly and penetrate to deep place by repeating the collision with tungsten atoms with fixed scattering angle in the case of perfect crystal. However, when holes exist in the target material, the repetition of the collisions with tungsten atoms stops at the hole. As a result, the incident helium atom deviate from its channeling path. This phenomenon is called dechanneling.

Figure 11 shows a typical trajectory of incident helium atoms move in tungsten material with holes. The helium atom moves straightly in vertical direction by channeling before the helium atom reaches to the hole (A in Fig. 11). When the helium atom reaches to the hole, the direction of helium atom is changed by causing large angle scattering (B in Fig. 11). After that, the helium atom moves straightly again (C in Fig. 11). Because of the dechanneling, the mean penetration depth decreases as the surface area increases.

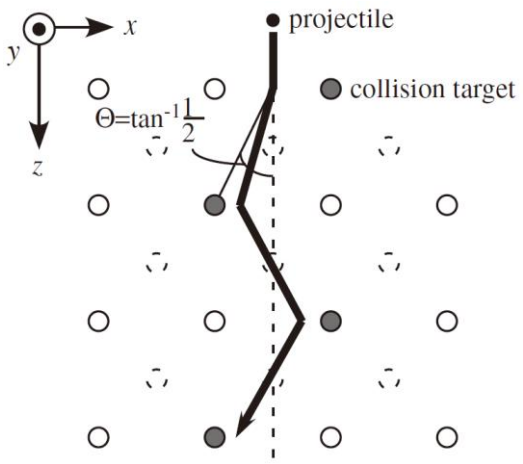

Fig. 10. Relation between the scattering angle Θ and the channeling path. [13]

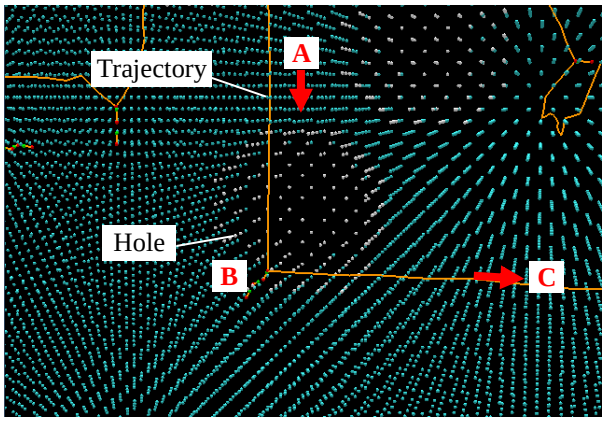

Fig. 11. Typical trajectory of the incident helium atom which occurred dechanneling at a hole.

6. Summary

BCA simulation of helium injection into bcc tungsten with nanoporous structure is performed. The mean penetration depth decreases as number of holes increases. From the trajectory analysis, it is found that the decrease of mean penetration depth of incident helium atoms is caused by the dechanneling at the holes.

Acknowledgments

Numerical simulations were carried out using the Plasma Simulator at the National Institute for Fusion Science, Japan.

This work is performed with the support and under the auspices of the NIFS Collaborative Research Programs (NIFS14KNTS043) and a Grant-in-Aid for Young Scientists (B) (No. 26790065) from the Ministry of Education, Culture, Sports, Science, and Technology, Japan.

References

[1] H. Iwakiri, K. Yasunaga, K. Morishita, and N. Yoshida, *J. Nucl. Mater.*, vol.283-287, p.1134, 2000.
[2] D. Nishijima, M.Y. Ye, N. Ohno, and S. Takamura, *J. Nucl. Mater.*, vol.329-333, p.1029, 2004.
[3] S. Takamura and Y. Uesugi, *Bulletin of Aichi Institute of Technology*, vol.50, p.94, 2015.
[4] M. Tokitani, N. Yoshida, K. Tokunaga, H. Sakakita, S. Tiyama, H. Koguchi, Y. Hirano, and S. Masuzaki, *Plasma Fusion Res.*, vol.5, p.012, 2010.
[5] S. Takamura, N. Ohno, D. Nishijima, and S. Kajita, *Plasma Fusion Res.*, vol.1, p.051, 2006.
[6] S. Kajita, T. Saeki, Y. Hirahata, M. Yajima, N. Ohno, R. Yoshihara, and N. Yoshida, *Jpn. J. Appl. Phys.*, vol.50, p. 08JG01, 2011.
[7] Y. Yamamura and Y. Mizuno, *Inst. Plasma Phys. Nagoya University*, IPPJ-AM-40, 1985.
[8] K. Ohya and R. Kawakami, *J. Appl. Phys.*, vol.5424, p. 40, 2001.
[9] J. P. Biersack and W. Eckstein, *Appl. Phys. A*, vol.73, p. 34, 1984.
[10] S. Saito, A. Takayama, A. M. Ito, A. Kenmotsu, and H. Nakamura, *Progress in Nuclear Science and Technology*, vol.2, p.44, 2011.
[11] S. Saito, A. Takayama, A. M. Ito, and H. Nakamura, *Proc. 30th JSST Annual Conference*, p.197, 2011.
[12] S. Saito, A. Takayama, A. M. Ito, and H. Nakamura, *Proc. 31st JSST Annual Conference*, p.46, 2012.
[13] S. Saito, A. M. Ito, A. Takayama, and H. Nakamura, *J. Nucl. Mater.*, vol.438, p.S895, 2013.
[14] S. Saito, M. Tokitani, and H. Nakamura, *Springer CCIS*, vol.474, p.176, 2014.
[15] G. Moliere, *Naturforsch*. 2A, p.133, 1947.